Articles

Synthesis and Characterization of Tp*MoOX$_2$ (X = F, Cl, Br; Tp* = Hydrotris(3,5-dimethylpyrazol-1-yl)borate)

Norriel S. Nipales and T. David Westmoreland*

Department of Chemistry, Wesleyan University, Middletown, Connecticut 06459

Received August 5, 1994[⊗]

Tp*MoOX$_2$ complexes (Tp* = hydrotris(3,5-dimethylpyrazol-1-yl)borate; X = F, Cl, Br) were synthesized by treatment of Tp*MoO(OCH$_3$)$_2$ with HX(aq) or HX(g) and characterized by infrared, EPR, and optical spectroscopies and by cyclic voltammetry. The IR of the complexes showed high $\nu_{Mo=O}$ stretching frequencies consistent with the relatively poor π-donating ability of the halides. The relative values of g_{iso} for the series was Br > Cl > F with an opposite trend in A_{iso}^{Mo}. Extensive ligand superhyperfine splitting was observed in the EPR spectra of frozen glasses of the fluoride and bromide complexes. Cyclic voltammetry exhibited quasi-reversible one-electron reductions with potentials that followed the trend Br > Cl ≫ F.

Introduction

The $\{Mo^VO\}^{3+}$ moiety continues to be of considerable relevance to the study of the active sites of molybdenum oxidoreductase enzymes.[1] The d^1 electronic structure of Mo(V) makes it especially suitable for characterization by EPR spectroscopy, and many spectra of oxidoreductase active sites and synthetic models have been published.[1e,2-5] The detailed relationships among EPR parameters, electronic structure, and coordination environment have not, however, been well defined. The best characterized cases[6,7] are based on ions such as $[MoOX_n]^{(n-3)-}$ (X = F, Cl, Br; n = 4, 5) which have relatively high symmetry (C_{4v}). In order to understand how low-symmetry effects are manifested in the EPR parameters, we have sought synthetically accessible low-symmetry $\{Mo^VO\}^{3+}$ complexes in which the ligands may be rationally and systematically varied.

The Tp*MoOXY series of complexes (Tp* = hydrotris(3,5-dimethylpyrazol-1-yl)borate anion; X, Y = variable ligands) is attractive since much of its synthetic chemistry has been established[8] and the complexes have low point group symmetries (C_s if X = Y, C_1 if X ≠ Y). Our focus here is on the dihalide systems (X = Y = F, Cl, Br). These complexes constitute a systematically varied series of related molecules in which trends in spectroscopic parameters and electronic structure can be explored. In many ways, these complexes represent a lower symmetry variant of the more thoroughly studied $[MoOX_n]^{(n-3)-}$ systems.[6,7] A detailed oriented single-crystal EPR study on Tp*MoOX$_2$ (X = Cl, SCN) has already appeared.[5b] The Tp*MoOX$_2$ series also provides good model systems for the study of ligand superhyperfine interactions, since their spectra exhibit fewer superhyperfine splittings than those of the tetrahalo species. We report here efficient synthetic routes to the previously unreported difluoride and dibromide complexes along with characterization of the new complexes by spectroscopic and electrochemical techniques.

Experimental Section

General Procedures. Organic solvents were dried over 3 Å molecular sieves prior to use. All other reagents were used as received. Dry HX (X = F, Cl, Br) gas was obtained by dropwise addition of concentrated HX(aq) to concentrated sulfuric acid. For X = Cl and Br, the evolved gas was also passed through a short Drierite column. The Tp*MoOCl$_2$ starting material was synthesized according to the literature procedure.[8a] Elemental analyses were performed by Atlantic Microlab, Inc., Atlanta, GA.

Tp*MoO(OCH$_3$)$_2$. Tp*MoO(OCH$_3$)$_2$ was synthesized by two different routes.

[⊗] Abstract published in *Advance ACS Abstracts,* May 15, 1995.

(1) (a) *Molybdenum and Molybdenum Containing Enzymes*; Coughlan, M., Ed.; Pergamon: New York, 1980. (b) *Molybdenum Enzymes*; Spiro, T. G., Ed.; Wiley-Interscience: New York, 1986. (c) Burgmayer, S. J.; Steifel, E. I. *J. Chem. Educ.* **1985**, *62*, 943-953. (d) Stiefel, E. I. *Prog. Inorg. Chem.* **1987**, *22*, 1-223. (e) Bray, R. C. *Q. Rev. Biophys.* **1988**, *21*, 299-329. (f) Wooton, J. C.; Nicolson, R. E.; Cock, J. M.; Walters, D. E.; Burke, J. F.; Doyle, W. A.; Bray, R. C. *Biochem. Biophys. Acta* **1991**, *1057*, 157-185. (g) *Molybdenum Enzymes, Cofactors, and Model Systems*; Steifel, E. I., Coucouvanis, D., Newton, W. E., Eds.; American Chemical Society: Washington, DC, 1993. (h) Enemark, J. H.; Young, C. G. *Adv. Inorg. Chem.* **1993**, *40*, 1-88.

(2) Cramer, S. P. *Adv. Inorg. Bioinorg. Mech.* **1983**, *2A*, 259-316.

(3) (a) George, G. N.; Bray, R. C. *Biochemistry* **1988**, *27*, 3603-3609. (b) Wilson, G. L.; Greenwood, R. J.; Pilbrow, J. R.; Spence, J. T.; Wedd, A. G. *J. Am. Chem. Soc.* **1991**, *113*, 6803-6812. (c) Greenwood, R. J.; Wilson, G. L.; Pilbrow, J. R.; Wedd, A. G. *J. Am. Chem. Soc.* **1993**, *115*, 5385-5392.

(4) George, G. N.; Prince, R. C.; Kipke, C. A.; Sunde, R. A.; Enemark, J. H. *Biochem. J.* **1988**, *256*, 307-309.

(5) (a) Collison, D.; Mabbs, F. E.; Enemark, J. H.; Cleland, W. E., Jr. *Polyhedron* **1985**, *5*, 423-425. (b) Collison, D.; Eardley, D. R.; Mabbs, F. E.; Rigby, K.; Bruck, M. A.; Enemark, J. H.; Wexler, P. A. *J. Chem. Soc., Dalton Trans.* **1994**, 1003-1011.

(6) (a) DeArmond, K.; Garrett, B. B.; Gutowsky, H. S. *J. Chem. Phys.* **1965**, *42*, 1019-1025. (b) Manoharan, P. T.; Rogers, M. T. *J. Chem. Phys.* **1968**, *49*, 5510-5519. (c) Dalton, L. A.; Bereman, R. D.; Brubaker, C. H., Jr. *Inorg. Chem.* **1969**, *8*, 2477-2480. (d) van Kemenade, J. T. C. *Recl. Trav. Chim. Pays-Bas* **1970**, *89*, 1100-1108. (e) van Kemenade, J. T. C. *Recl. Trav. Chim. Pays-Bas* **1973**, *92*, 1102-1120. (f) Radhakrishna, S.; Chowdari, B. V. R.; Viswanath, A. K. *Chem Phys. Lett.* **1975**, *30*, 231-234. (g) Radhakrishna, S.; Chowdari, B. V. R.; Viswanath, A. K. *Chem. Phys. Lett.* **1976**, *42*, 319-322. (h) Garner, C. D.; Hill, L. H.; Mabbs, F. E.; McFadden, D. L.; McPhail, A. T. *J. Chem. Soc., Dalton Trans.* **1977**, 853-858.

(7) Balagopalakrishna, C.; Kimbrough, J. T.; Westmoreland, T. D. Manuscript in preparation.

(8) (a) Cleland, W. E., Jr.; Barnhart, K. M.; Yamanouchi, K.; Collison, D.; Mabbs, F. E.; Ortega, R. D.; Enemark, J. H. *Inorg. Chem.* **1987**, *26*, 1017-1025. (b) Chang, C.-S. J.; Enemark, J. H. *Inorg. Chem.* **1991**, *30*, 683-688.

0020-1669/95/1334-3374$09.00/0

(A)[9] To a solution of 0.65 g (1.35 mmol) of Tp^*MoOCl_2 in 175 mL of methanol was added 2.60 g of NaOH pellets. The mixture was stirred overnight (~12 h) at 40 °C and filtered. The solvent was removed by rotary evaporation to give a blue-green solid, which was subsequently recrystallized by slow evaporation of a toluene solution. The yield was 0.6020 g (1.28 mmol, 94.8%). All properties (IR, EPR, UV−vis, electrochemistry) agree with those previously reported.[8a]

(B) A 0.50 g (9.25 mmol) portion of NaOMe was added to a mixture of 2.00 g (4.17 mmol) of Tp^*MoOCl_2 in 100 mL of methanol. A small portion (<2 g) of mossy zinc was added, and the mixture was stirred at 40 °C for 2 h. The mixture was filtered, and the solvent was removed on a rotary evaporator. The product was purified by column chromatography on neutral alumina using dichloromethane as eluant. A 1.95 g (4.13 mmol) quantity of the blue-green product was obtained (99% yield).

Tp^*MoOF_2. A 0.2219 g (0.4710 mmol) sample of $Tp^*MoO(OCH_3)_2$ was dissolved in 40 mL of dichloromethane. Dry HF(g) was bubbled through the $Tp^*MoO(OCH_3)_2$ solution at a rate of approximately 45 mL/min. The solution immediately turned bright green. After an additional hour of bubbling HF gas, the solvent was vacuum-evaporated to yield a bright green solid (0.1204 g, 57.2% yield based on $Tp^*MoO(OCH_3)_2$). The solid compound slowly decomposes to EPR-silent products which are as yet unidentified. All characterization data reported below were obtained on freshly prepared samples. Due to decomposition, a satisfactory elemental analysis was not obtained.

Tp^*MoOCl_2 *via* the Dimethoxy Complex. HCl gas was bubbled through a solution of 0.2178 g (0.4623 mmol) of $Tp^*MoO(OCH_3)_2$ in 25 mL of methanol. The color changed from blue-green to green, and a precipitate formed. The mixture was stirred for 1 h and then filtered, giving 0.2159 of green solid (97.3% yield). All properties agreed with those of an authentic sample.

Tp^*MoOBr_2. (A) A methanol solution of 0.2058 g (0.4368 mmol) $Tp^*MoO(OCH_3)_2$ was treated with HBr(g) for 1 h. The mixture turned from blue-green to brown. It was then filtered, and the filtrate was evaporated to dryness. A 0.2060 g quantity of brown solid was obtained (80.2% yield).

(B) To a solution of 0.4879 g (1.03 mmol) of $Tp^*MoO(OCH_3)_2$ in 50 mL of methanol was added 5.00 mL of concentrated HBr(aq). The mixture was stirred for 2 h, during which a precipitate formed. The brown mixture was filtered, giving a yellow-brown solid and a brown filtrate. The solid was washed with methanol and then dried under vacuum. The yield was 0.2549 g (44% based on $Tp^*MoO(OCH_3)_2$). Anal. Calcd for $C_{15}H_{22}N_6Br_2BMo$: C, 31.66; H, 3.89; N, 14.77. Found: C, 32.40; H, 4.03; N, 14.66.

Physical Measurements. Infrared spectra were obtained in KBr pellets using a Perkin-Elmer 1600 FTIR spectrometer. Optical spectra were obtained in dichloromethane solutions with a Hewlett Packard 8451A diode array spectrophotometer. Electron paramagnetic resonance spectra were obtained at X-band frequencies with a Bruker ESP 300 spectrometer. Spectra of frozen glasses were obtained at 77 K using an immersion finger dewar. Simulated EPR spectra were calculated using a modified version of QPOW.[10] Cyclic voltammetric measurements were obtained using an EG&G potenstiostat−galvanostat, Model 250. All electrochemical experiments were performed in dichloromethane using $[Bu_4N][BF_4]$ as electrolyte at a platinum disk electrode and were referenced to SSCE.

Results and Discussion

$Tp^*MoO(OCH_3)_2$ has been previously prepared by treatment of Tp^*MoOCl_2 with $NaOCH_3$ in toluene.[8a] We have used two new synthetic approaches which give higher yields and higher purity of the complex. Method A, eq 1, involves direct

$$Tp^*MoOCl_2 \xrightarrow[CH_3OH]{NaOH} Tp^*MoO(OCH_3)_2 \qquad (1)$$

substitution of Cl^- by OCH_3^-, similar to the original synthesis. In fact, the reaction proceeds essentially identically if $NaOCH_3$ is employed as the base rather than NaOH. Method B, eq 2,

$$Tp^*MoOCl_2 \xrightarrow[CH_3OH]{NaOCH_3/Zn} Tp^*MoO(OCH_3)_2 \qquad (2)$$

provides the same product with a slightly higher yield over a shorter time. For route B, there is evidence that reduction of a portion of the Tp^*MoOCl_2 generates a catalytic species which accelerates the substitution reaction. The most likely scenario is outlined in the following scheme:

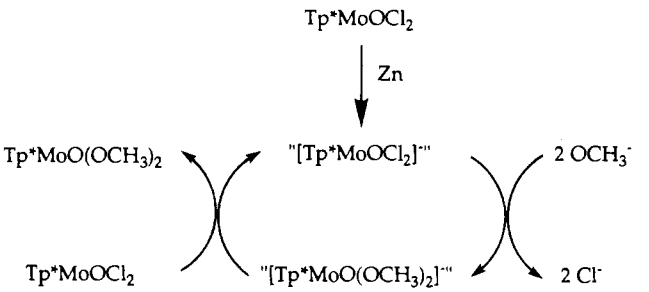

In the proposed scheme, Tp^*MoOCl_2 is reduced by Zn(s) to a Mo(IV) species which is more substitutionally labile than the Mo(V) starting material. The excess of $NaOCH_3$ drives the substitution of both Cl^- ligands. The very negative $E_{1/2}$ for the Mo(V/IV) couple of the dimethoxy species (−1.100 V vs SCE)[8a] indicates that $[Tp^*MoO(OCH_3)_2]^-$ is a very good reductant. The potential of Tp^*MoOCl_2 (−0.251 V vs SCE)[8a] provides a very favorable driving force for reduction by the reduced dimethoxy complex to regenerate the putative catalytic Mo(IV) species. In support of this scheme, it should be noted that exhaustive reduction of a solution of Tp^*MoOCl_2 and $NaOCH_3$ in CH_3OH can be achieved by extensive reaction with Zn/Hg amalgam. When one drop of the resulting solution is added to approximately 10 mL of a fresh solution of Tp^*MoOCl_2 in CH_3OH, conversion to the dimethoxy complex occurs spontaneously with yields of >50%. In the absence of the reduced solution, no conversion is observed.

The general synthetic scheme for the Tp^*MoOX_2 series takes advantage of the basicity of the coordinated methoxy ligands. We have found that treatment of $Tp^*MoO(OCH_3)_2$ with a variety of HA results in the protonation and loss of the methoxy ligands and coordination of HA. It should be noted that Cleland *et al.*[8a] have used a similar approach to Tp*MoOXY complexes via the ethylene glycolate complex. In our hands, synthesis of these complexes via the dimethoxy derivative, as described above, gives considerably higher overall yields and the products require fewer subsequent purification steps. The routes appear to be general, as demonstrated by our ability to synthesize not only known complexes, e.g. Tp^*MoOCl_2, but also new complexes with H_2SO_4, H_3PO_4, and RCOOH.[11] In particular, the complexes Tp^*MoOX_2 (X = F, Cl, Br) can be synthesized in high yields by treating a solution of $Tp^*MoO(OCH_3)_2$ in methylene chloride with HX gas, giving yields typically greater than 80%. Tp^*MoOCl_2 and Tp^*MoOBr_2 can also be synthesized by treating $Tp^*MoO(OCH_3)_2$ with gaseous HCl or HBr (or concentrated HBr(aq)) in methanol. Under these conditions the products precipitate directly from the reaction mixture in yields of >50%.

Infrared Spectroscopy. There are two principal diagnostic IR bands for Tp^*MoOX_2 complexes, a Mo=O stretch ($\upsilon_{Mo=O}$) in the 900−1000 cm^{-1} region[8] and a terminal B−H stretch

(9) Wedd, A. G. Personal communication.

(10) (a) Nilges, M. J. Ph.D. Thesis, University of Illinois, Urbana, IL, 1979. (b) Belford, R. L.; Nilges, M. J. Computer Simulation of Powder Spectra. *Abstracts of Papers*; EPR Symposium, 21st Rocky Mountain Conference, Denver, CO, 1979. (c) Maurice, A. M. Ph.D. Thesis, University of Illinois, Urbana, IL, 1982.

(11) Nipales, N. S.; Westmoreland, T. D. Unpublished results.

Table 1. Selected Properties of Tp^*MoOX_2 Complexes

	Tp^*MoOF_2	Tp^*MoOCl_2[a]	Tp^*MoOBr_2
$\upsilon_{Mo=O}$ (cm^{-1})	964.3	962.0	961.1
υ_{B-H} (cm^{-1})	2550.3	2558.5	2559.5
g_{iso}[b]	1.9331	1.9464	1.9746
A_{iso}^{Mo} (10^{-4} cm^{-1})[b]	51.0	46.4	43.4
A_{iso}^{L} (10^{-4} cm^{-1})[b]	21.7	c	c
g_1	1.977	1.971	2.042
g_2, g_3	1.920, 1.904	1.944, 1.932	(1.94)[d]
A_1^{Mo} (10^{-4} cm^{-1})	50.0	43.7	60.0
$A_{(1,2,3)}^{L}$ (10^{-4} cm^{-1})	(21.3, 16.0, 18.0)[e]	c	(39.6)[e,f]
λ_{max} (ϵ)[g]	686.0 (32)	706.0 (48)	676.0 (151)
(nm (M^{-1} cm^{-1}))	450.0 (74)	438.0 (1000) sh	390.0 (2638) sh
	334.0 (855) sh	336.0 (3732) sh	300.0 (8515) sh
	262.0 (4395)	280.0 (10 262)	230.0 (8664)
	224.0 (11 070)	228.0 (9880)	
$E_{1/2}$ (V)[h]	−0.888	−0.290	−0.186
$E_p^{an} - E_p^{cath}$ (V)[i]	0.158	0.079	0.078
(i_p^a/i_p^c)[i]	0.692	0.986	0.960

[a] All values are within 1% of those previously reported.[5,8a] [b] In toluene. [c] Not resolved. [d] Average of g_2 and g_3 estimated from g_{iso} and g_1. [e] Estimated directly from the low-temperature spectrum. [f] Average spacings of most prominent ligand hyperfine features. [g] In dichloromethane. [h] Average of E_p^{an} and E_p^{cath} vs SSCE. [i] At 10 mV/s for the chloride and the bromide; at 50 mV/s for the fluoride.

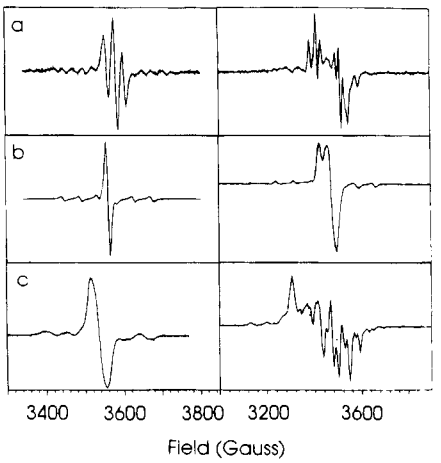

Figure 1. Room-temperature (left) and 77 K (right) X-band EPR spectra in toluene of (a) Tp^*MoOF_2, (b) Tp^*MoOCl_2, and (c) Tp^*MoOBr_2.

(υ_{B-H}, 2450−2650 cm^{-1})[12] from the Tp* ligand. Table 1 gives $\upsilon_{Mo=O}$ and υ_{B-H} for the halide complexes. Tp*MoOXY complexes (where X and Y are variable ligands) in general exhibit $\upsilon_{Mo=O}$ between 910 and 960 cm^{-1}, and it has been previously noted that the frequencies tend to scale inversely as the π-donating ability of the ligands.[8a] This suggests that the strength of the Mo=O bond is significantly affected by the π-donating ability of the variable ligands. The similar and high values $\upsilon_{Mo=O}$ for the Tp^*MoOX_2 series are consistent with the relatively poor overall π-donating ability of the halides. Only small variations in υ_{B-H} are observed in the series and indicate the insensitivity of the Tp*−Mo bonding to changes in the bound halide.

EPR Spectroscopy. The EPR spectra at X-band frequencies of the halide complexes at room temperature and in frozen toluene are shown in Figure 1. In each spectrum, molybdenum hyperfine structure from the $^{95/97}Mo$ isotopes ($I_N = {}^5/_2$, 25% natural abundance) is clearly apparent. Additional superhyperfine features are resolved in both of the Tp^*MoOF_2 spectra as well as in the low-temperature spectrum of Tp^*MoOBr_2. The g values and the values of the isotropic molybdenum hyperfine and isotropic ligand superhyperfine splittings from simulations are given in Table 1. Complete simulation parameters and figures of the simulated solution spectra are included in the supplementary material. With the exception of that of Tp^*MoOCl_2, the low-temperature spectra have proved too complex for satisfactory powder patterns to be simulated. Although the full definition of the anisotropic parameters of the difluoro and dibromo complexes awaits the results of oriented single-crystal studies,[13] estimates of some anisotropic parameters are also given in Table 1. A number of trends are evident in the data. The g values of the complexes vary in the order F < Cl < Br. The origin of this trend is a combination of (1) increasing covalency of the ground and ligand field excited states, (2) increasing contributions from low-lying ligand to metal charge transfer excited states, and (3) increasing ligand spin−orbit coupling. Similar trends have been observed,[6] and the origin has been quantitatively demonstrated[7] for the $[MoOX_n]^{(n-3)-}$ series.

The values of the isotropic molybdenum hyperfine coupling constants follow the trend F > Cl > Br. In the $[MoOX_n]^{(n-3)-}$ series, it has been demonstrated that the molybdenum hyperfine coupling is dominated by Fermi contact and an approximately linear relationship has been proposed between the metal character in the ground state and the isotropic molybdenum hyperfine coupling constant.[7] Assuming a similar proportionality, ground state metal character in the Tp^*MoOX_2 series quantitatively decreases in the order F(~89%) > Cl(~86%) > Br(~84%).

Superhyperfine features which arise from the interaction of the ligand nuclear spin with the unpaired electron were observed in the room-temperature spectrum of the fluoride complex and in the low-temperature spectra of both the fluoride and the bromide complexes. The splittings depend both on the nuclear g value and on the unpaired spin density at the ligand. Since chlorine has a relatively small g_N (^{35}Cl = +0.548, ^{37}Cl = +0.456), splittings due to $^{35,37}Cl$ are not resolved even at 77 K. Fluorine has a much larger g_N (^{19}F = +5.258), and the splittings are observed in fluid solution. A detailed analysis of the ligand superhyperfine splittings will be the subject of a future paper.[13]

UV−Visible Absorption Spectra. The UV−visible spectra of the compounds in dichloromethane are summarized in Table 1. The lowest energy band (675−710 nm) for each complex is relatively weak and is consistent with a ligand field assignment, as previously suggested for related complexes.[8a] The lowest energy band for the bromide complex has a somewhat higher molar absorptivity, suggesting some charge transfer character as well in this transition. All three complexes exhibit a transition in the 230−240 nm region which is also present for other complexes containing Tp* (e.g., Tp^*SnX_3) and for the free ligand.[11] This band is assigned as an intraligand transition of the Tp* ligand. The relatively intense absorptivity in the 300−500 nm region of each complex is most likely due to ligand-to-metal charge transfer transitions, but detailed assignments of these bands will require more sophisticated spectroscopic studies. For Tp^*MoOCl_2 such a detailed study was recently published[14] and confirms the presence of several LMCT transitions in the visible region. In general, it appears that the LMCT manifold shifts to lower energy down the series X = F, Cl, Br, as expected on the basis of the increasing ease of oxidation of the halide.

(12) Nakamoto, K. *Infrared and Raman Spectra of Inorganic and Coordination Compounds*; John Wiley and Sons: New York, 1986.

(13) Nipales, N. S.; Westmoreland, T. D. Work in progress.

(14) Carducci, M. D.; Brown, C.; Solomon, E. I.; Enemark, J. H. *J. Am. Chem. Soc.* **1994**, *116*, 11856−11868.

Electrochemistry. Cyclic voltammetric data for the complexes were obtained in dichloromethane and are summarized in Table 1. The chloride and bromide complexes exhibited quasi-reversible ($i_p^a/i_p^c \cong 1.0$) one-electron reductions corresponding to the Mo(V/IV) couple. For the fluoride complex $i_p^a/i_p^c \cong 0.7$ with a 50 mV/s scan rate and is a function of scan rate. The value begins to approach 1.0 at slower scan rates but is complicated by subsequent irreversible reactions. The $E_{1/2}$ values for the complexes indicate that the relative ease of reduction is Br > Cl ≫ F. It is not clear why the reduction of the fluoride complex is so dramatically negative relative to the other two complexes. This trend may reflect a greater effective π-donation of fluoride to the orbital containing the unpaired electron. Such enhanced π-donating properties were recently noted in other systems.[15] In light of the small differences in $\upsilon_{Mo=O}$ discussed above, these results suggest a large anisotropy of π-donor interactions from the halide. The increased π-donating ability of fluoride may relate to a shorter Mo−F bond length. In high-valence Mo−halide complexes, Mo−F bonds are typically 0.5 Å shorter than the Mo−Cl bonds in the analogous complexes.[16] Well-defined Mo(VI/V) couples were not observed. In the dichloro and dibromo complexes, irreversible oxidative waves were observed near the solvent limit (+1.2 V vs SSCE).

Concluding Remarks

Efficient synthetic routes to a homologous series of halide derivatives of Tp*MoOX$_2$ have been developed. These complexes in general have the expected physical properties, with the exception of the reduction potential of Tp*MoOF$_2$. In particular, these complexes exhibit clear trends in spectroscopic properties which provide a basis for exploring the detailed relationship between EPR parameters and electronic structure for low-symmetry $\{MoO\}^{3+}$ sites.

Acknowledgment. The authors gratefully acknowledge the donors of the Petroleum Research Fund, administered by the American Chemical Society, and the National Institutes of Health for support.

Supplementary Material Available: A listing of EPR simulation parameters and figures showing room-temperature solution EPR simulations and cyclic voltammograms for Tp*MoOX$_2$ (X = F, Cl, Br) (5 pages). Ordering information is given on any current masthead page.

IC940930H

(15) (a) Poulton, J. T.; Folting, K.; Streib, W. E.; Caulton, K. G. *Inorg. Chem.* **1992**, *31*, 3190−3191. (b) Hauger, B.; Gusev, D.; Caulton, K. G. *J. Am. Chem. Soc.* **1994**, *116*, 208−214. (c) Bickford, C. C.; Johnson, T. J.; Davidson, E. R.; Caulton, K. G. *Inorg. Chem.* **1994**, *33*, 1080−1086. (d) Poulton, J. T.; Sigalas, M. P.; Folting, K.; Streib, W. E.; Eisenstein, O.; Caulton, K. G. *Inorg. Chem.* **1994**, *33*, 1476−1485.

(16) For example, compare $MoOF_4$, $\langle Mo-F_t\rangle$ = 1.82 Å,[a] with $MoOCl_4$, $\langle Mo-Cl_t\rangle$ = 2.32 Å.[b] (a) Edwards, A. J.; Steventon, B. R. *J. Chem. Soc. A* **1968**, 2503−2510. (b) Taylor, J. C.; Waugh, A. B. *J. Chem. Soc., Dalton Trans.* **1980**, 2006−2009.